

Absence of weak electron localization in epitaxial Fe wires on GaAs(110)

C. Hassel,* F. M. Römer, G. Dumpich, and J. Lindner

Fachbereich Physik, Experimentalphysik, AG Farle, Universität Duisburg-Essen, 47048 Duisburg, Germany

(Received 31 October 2008; revised manuscript received 23 January 2009; published 24 March 2009)

We measured the low-temperature magnetoresistance of epitaxial Fe wires on GaAs(110) for wires with widths ranging from 100 to 3000 nm. All wires exhibit a logarithmic resistance increase toward lower temperatures. The resistance increase is independent of the external magnetic field applied perpendicular to the film plane. This behavior shows that the logarithmic resistance increase is due to electron-electron interaction rather than weak localization effects. By decreasing the wire width we find that the temperature dependence of the resistance increases which is due to a $2d-1d$ transition of the electron-electron interaction.

DOI: [10.1103/PhysRevB.79.092417](https://doi.org/10.1103/PhysRevB.79.092417)

PACS number(s): 73.63.-b, 73.20.Fz, 75.47.-m

I. INTRODUCTION

The low-temperature magnetoresistance properties of various nonmagnetic metallic films and wires have been intensively investigated during the past decades. Essentially, two different quantum mechanical corrections to the resistance explain the experimentally found resistance increase toward low temperatures. One model concerns the phase coherent backscattering of noninteracting electrons called weak electron localization (WEL).¹ The other model originates from a modified screening of electrons due to diffuse electron scattering and is called enhanced electron-electron interaction (EEI).² For two-dimensional systems, both effects result in a logarithmic resistance increase for low temperatures. To distinguish these effects external magnetic fields are applied perpendicular to the film plane. Via the Aharonov Bohm effect, the vector potential acts on the phase of the electron waves.^{3,4} It has been shown that already small magnetic fields are sufficient to destroy the phase coherence on length scales of $L_\phi = (\hbar/4eB\phi)^{1/2}$ and thus lower the logarithmic resistance increase.⁵ In contrast, the EEI is hardly modified by magnetic fields of the order of 1 T.⁶

So far, many groups have addressed the question both experimentally and theoretically as to whether or not WEL effects also survive in magnetic systems⁷⁻¹⁵ since internal magnetic fields in *ferromagnetic* films or wires may or may not influence the phase coherence between conduction electrons even in the absence of external magnetic fields. Dugaev *et al.*¹⁶ have shown in their theoretical work that the magnetic induction for two-dimensional in-plane magnetized materials does not break the phase coherence and thus this magnetization does not affect the localization correction. Aliev *et al.*¹⁷ have shown that in antiferromagnetically coupled multilayers antilocalization effects are suppressed in the presence of domain walls. For ferromagnetic epitaxial GaMnAs wires effects of weak antilocalization were found both for two-dimensional and one-dimensional systems at very low temperatures in the mK range.¹⁸ On the other hand, in various experimental investigations for “conventional” ferromagnetic films and wires at low temperatures direct evidence of the presence of weak electron localization could not be found.^{19,20} The absence of weak localization effects was explained by Sil *et al.*²¹ by the fact that domain wall scattering destroys WEL, which is predominantly present in polycrys-

talline samples being magnetically inhomogeneous.

In the present Brief Report we study the low-temperature magnetoresistance of epitaxial Fe wires on GaAs(110) with varying widths in the range between 100 and 3000 nm. Due to the epitaxial structure of the wire, the magnetic state in remanence is more homogeneous than for polycrystalline samples and one would expect that for these wires quantum contributions arising from WEL should be observable. However, also for these samples we do not find a contribution of weak electron localization for wires. Our data can be well explained in the framework of enhanced electron-electron interaction.

II. EXPERIMENTAL DETAILS

Epitaxial Fe wires on GaAs(110) are prepared from continuous Fe films prepared in a ultrahigh vacuum chamber with a base pressure of $p = 1 \times 10^{-10}$ mbar. Prior to the Fe evaporation from a rod with a purity of 99.999%, the GaAs(110) substrates are cleaned in a combined annealing/sputtering process. The Fe film has a thickness of 10 nm. The structure of the substrate and the film is investigated by low-energy electron diffraction. From these investigations the epitaxial relation GaAs(110)[001]||Fe(110)[001] was derived. Finally, the films are capped with Ag and Pt to avoid oxidation in the *ex situ* preparation steps. The conductivity of the cap layer is much smaller than that of the Fe wires as was proven with measurements on the pure buffer so that the transport is dominated by the Fe wire. The anisotropy parameters of the film are determined using ferromagnetic resonance proving that the magnetocrystalline easy direction as well as the easy direction of an additional uniaxial anisotropy points along the [001] direction. Subsequently, the films are structured into wires in an electron beam lithography process followed by Ar-ion sputtering. Details on the fabrication and characterization process are published elsewhere.²² Figure 1 shows an exemplary secondary electron micrograph of a typical sample structure. The Fe wire (from left to right) is contacted with four nonmagnetic gold wires to avoid an influence to the sample magnetization. The two outermost wires are used to inject the current into the wire; the inner contacts are used to measure the voltage. Magnetic images in remanence are taken in a D3000 magnetic force microscope (MFM) with commercially available MESP (magnetic etched

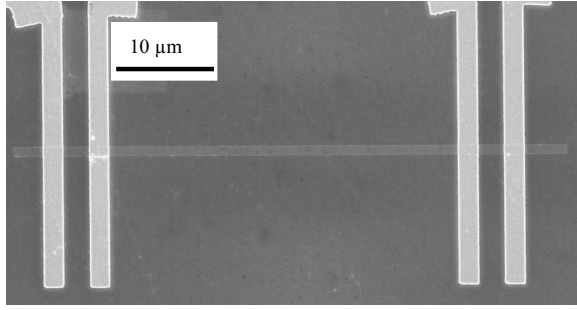


FIG. 1. Secondary electron micrograph of a contacted epitaxial Fe wire on GaAs(110).

silicon probes, Veeco Probes) tips after saturation of the wires in the [001] direction. Magnetoresistance measurements are carried out in a ⁴He bath cryostat with a commercial ac resistance bridge (LR700). The temperature can be varied between 1.4 and 300 K. The currents used for the measurements are kept below 1 μA for wires with a width of 3000 nm to avoid heating effects. For smaller wires the current was further reduced. The resolution of the setup is in the order of ΔR/R=10⁻⁶ at low temperatures.²³

III. RESULTS AND DISCUSSION

Figures 2 and 3 show MFM images in remanence after applying an external field in the [001] direction. Since we use an out-of-plane magnetized tip, only stray field compo-

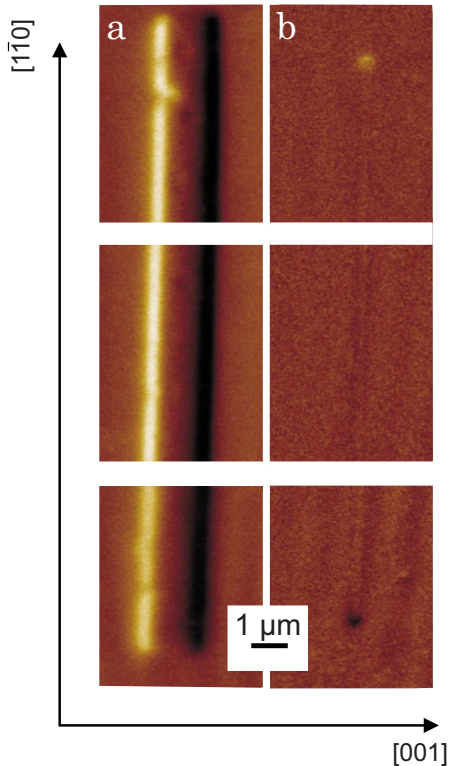


FIG. 2. (Color online) Remanent state after saturation of the wires in the easy direction for wires parallel to the $[1\bar{1}0]$ direction with a width of (a) 200 nm and (b) 2000 nm.

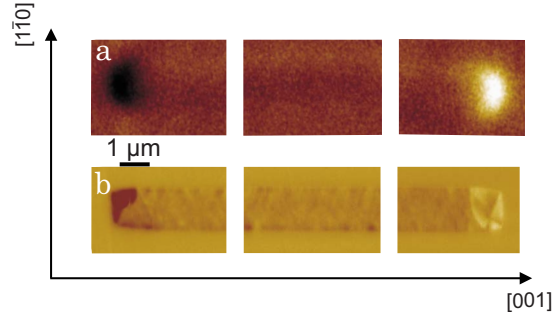


FIG. 3. (Color online) Remanent state after saturation of the wires in the easy direction for (a) a 2 μm wide epitaxial Fe wire parallel to the [001] direction and (b) a 2 μm wide polycrystalline Co wire (taken from Ref. 20).

nents pointing out of the film plane are detected. Figure 2(a) shows a 2 μm wide wire, with its long axis parallel to the $[1\bar{1}0]$ direction. The easy crystallographic direction is pointing transverse to the long wire axis. One can clearly see that we observe for the whole length of the wire a dark contrast on one side of the wire and a white contrast on the other side of the wire, which means that the magnetization is in remanence transverse to the long wire axis due to the crystalline anisotropy being larger than the shape anisotropy. This finding could be also confirmed by simulations with the object oriented micromagnetic framework (OOMMF).^{22,24} For a wire with a width of 200 nm we observe a different behavior [see Fig. 2(b)]. Here, only two poles at the end of the wire are detected indicating that the magnetization is longitudinally oriented in the wire, which is due to the fact that for small wires the shape anisotropy becomes larger as the crystalline anisotropies. Again this was confirmed by OOMMF simulations. Figure 3(a) shows a MFM image of a wire which is oriented parallel to the magnetocrystalline easy direction, so that both the shape and the crystalline anisotropy favor the same magnetization direction. One can clearly see that only at the ends of the wire poles are visible, but almost no contrast can be seen in the middle part of the wire. From that we can conclude that we have a homogeneous magnetization pointing in this direction. For comparison, Fig. 3(b) shows a MFM image of a polycrystalline Co wire from Ref. 20. Here, one can also see poles at the end of the wires, but domain formation was observed in the center region of the wire due to its polycrystalline nature.

Figure 4 shows the electrical resistance of a 3 μm wide Fe wire oriented parallel to the [001] direction at low temperatures for various external fields applied perpendicular to the film plane. One can clearly see that the resistance increases for all external fields logarithmically toward lower temperatures. At a temperature of 8 K the resistance reaches a minimum and increases linearly to higher temperatures. By varying the external magnetic field, we find that the curves are shifted to lower resistances. This is due to the fact that the magnetization slowly rotates out of the film plane and thus the overall resistance is reduced due to the anisotropic magnetoresistance.²⁵ However, the logarithmic slope of the resistance increase toward lower temperatures is the same for all applied magnetic fields. From this we conclude that no

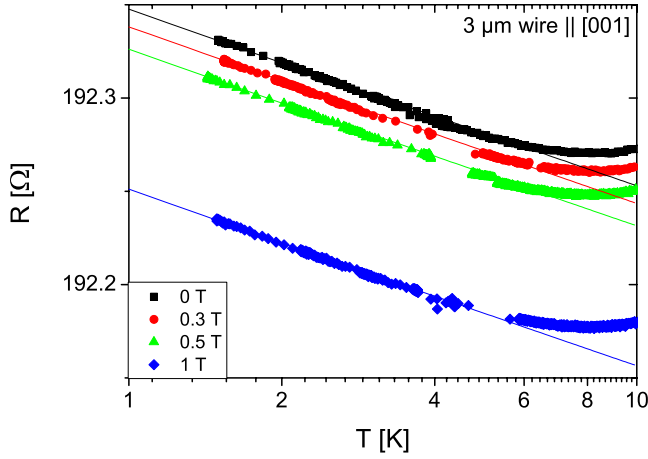


FIG. 4. (Color online) Resistance as a function of the logarithm of the temperature of a 3 μm wide epitaxial Fe wire oriented parallel to the [001] direction for various external fields applied perpendicular to the film plane.

effects of WEL are present in this epitaxial Fe wire. However, also EEI effects are known to cause a logarithmic resistance increase at low temperatures. The solid lines represent fits to the logarithmic resistance increase at low temperatures according to a formula developed by Neuttiens *et al.*²⁶ to describe the EEI in the transition region between two-dimensional and one-dimensional behavior, which is as follows:

$$\delta G_{\text{EEI}}^{1d-2d}(T) = \frac{\alpha}{\pi\hbar} \sum_{n=0}^{\infty} \frac{1}{\sqrt{\frac{w^2}{L_T^2} + (n\pi)^2}} - \frac{1}{\sqrt{\frac{w^2}{L_{T_0}^2} + (n\pi)^2}}. \quad (1)$$

Here, α is a screening factor introduced by Neuttiens *et al.*,²⁶ and L_T is the thermal diffusion length $L_T = \sqrt{\frac{\hbar D}{k_B T}}$ with the diffusion constant D . L_{T_0} is the thermal diffusion length at a reference temperature T_0 . As one can see from Fig. 4, the logarithmic resistance increase can be well fitted by Eq. (1).

To compare the data with other measurements, we calculate the change in the conductance over one decade of the temperature

$$\Delta G(10) = G_{\square}(10 \text{ K}) - G_{\square}(1 \text{ K}) = \frac{R_{\square}(1 \text{ K}) - R_{\square}(10 \text{ K})}{R_{\square}^2(10 \text{ K})},$$

whereby R_{\square} denotes the resistance per square of the wire and $R_{\square}(1 \text{ K})$ and $R_{\square}(10 \text{ K})$ are the extrapolated values of $R(T)$ according to the solid lines in Fig. 4 at 1 K and 10 K, respectively. $\Delta G(10)$ is thus proportional to the slope of the resistance increase. Obviously, the resistance above 6 K deviates from the straight lines in Fig. 4 indicating that electron-phonon interactions start to play a role. Our discussion and interpretation of the resistance data rely on data below 6 K. We find for the epitaxial Fe wire presented in Fig. 4 a value of $\Delta G(10) = 3 \times 10^{-5} \Omega^{-1}$, which is in good agreement with measurements for EEI in two-dimensional poly-

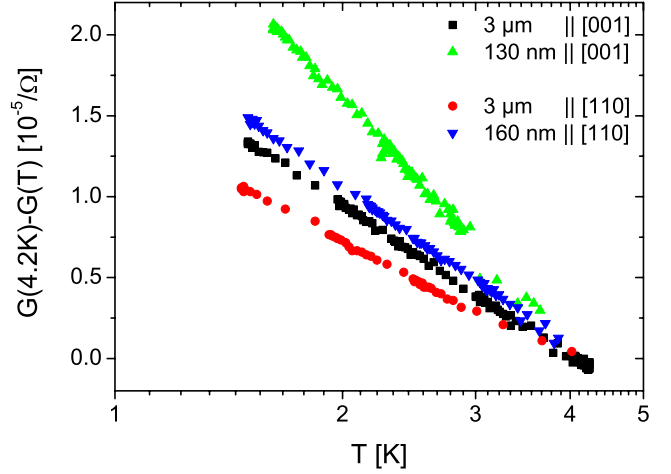


FIG. 5. (Color online) Relative change in the conductance of different epitaxial Fe wires as a function of the temperature.

crystalline Co wires.²³ The calculations from Sil *et al.* show that WEL should be present in the case of a homogeneous magnetization, which is the case for our wires as the MFM images clearly show. The effect should be smaller as compared to the EEI effects [$\Delta G(10)_{\text{WEL}} \approx 1 \times 10^{-5} \Omega^{-1}$], but this would still be clearly visible within our sensitivity.

To further investigate the WEL/EEI effects in ferromagnetic Fe wires, we prepared epitaxial Fe wires of different widths and also different orientations. Figure 5 shows the change in the conductance $\delta G(T) = G(4.2 \text{ K}) - G(T)$ for epitaxial Fe wires of two different orientations and widths at zero magnetic field. As one can see, we find a logarithmic conductance behavior with different slopes $\Delta G(10)$, which can be determined by extrapolating the straight line to 1 and 10 K, for the various epitaxial Fe wires, whereby the slope is steeper for smaller wires. Applying an external magnetic field perpendicular to the film plane, we find for the four Fe wires that their slopes are independent of the field strengths, as is shown, e.g., for the sample with $w = 3 \mu\text{m}$ parallel to the [001] direction in Fig. 4. Since we observe no magnetic field dependence, WEL effects are clearly not present for our epitaxial wires. Nevertheless, our results are in good agreement with theoretical calculations for EEI.

To investigate the widths' dependence on the conductance behavior of the epitaxial Fe wires arising from EEI, Fig. 6 shows $\Delta G(10)$ —corresponding to the slope of the $G(T)$ curves in Fig. 5—as a function of wire widths for epitaxial Fe wires of different orientation (parallel to [001] or $[\bar{1}10]$) as well as for polycrystalline wires.²³ For wider wires ($w > 1 \mu\text{m}$) the value of $\Delta G(10) = 3 \times 10^{-5} \Omega^{-1}$ is almost independent of the wire widths and close to the value we also look for polycrystalline Co wires in the 2d limit.²³ Note that there is only a slight difference of $\Delta G(10)$ for epitaxial Fe wires of different orientations. For decreasing wire widths ($w < 1 \mu\text{m}$) $\Delta G(10)$ is increasing to larger values. This can be well explained by a crossover from 2d to 1d behavior with respect to EEI. To show that our experimental data can be described by EEI, we calculated $\Delta G(10) = G(10 \text{ K}) - G(1 \text{ K})$ with Eq. (1) using $\alpha = 1.0$ and $D = 9.8 \times 10^{-4} \text{ m}^2/\text{s}$. The values of $\Delta G(10)$ are shown in Fig. 6 as a

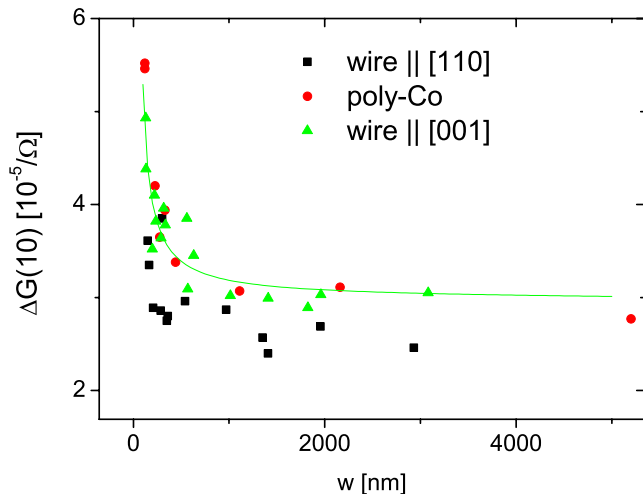


FIG. 6. (Color online) $\Delta G(10)$ values of various oriented epitaxial Fe wires and polycrystalline Co wires (from Ref. 20) as a function of the width of the wire.

solid green line. As one can see, there is reasonable agreement between our experimental data and theoretical calculations proving that indeed a transition from $2d$ to $1d$ behavior occurs. However, we also find slight differences between our data with respect to the wire orientation which might be due

to their different magnetization direction. The analysis of the data in Fig. 6 clearly shows that for epitaxial Fe wires effects based on EEI are almost independent of the microstructure of the ferromagnetic wire (polycrystalline/epitaxial) and only slightly dependent on their magnetic structures. Effects based on WEL are not present, independent of whether the magnetic structures are inhomogeneous or homogeneous.

Neumaier *et al.*¹⁸ observed weak antilocalization in ferromagnetic GaMnAs. However, GaMnAs has a very low magnetization compared to Fe. Further work should be done with materials with a magnetization value between these ones to investigate the influence of an increasing magnetization.

In conclusion, we have shown that for epitaxial Fe wires no effects of weak electron localization are present for temperatures down to $T=1.4$ K. The observed resistance increase toward low temperature can be explained by enhanced electron-electron interaction effects. Furthermore, for decreasing wire widths, we observe an increase in the slope of the resistance increase due to a transition from two-dimensional to one-dimensional behavior with respect to electron-electron interaction.

ACKNOWLEDGMENT

We thank the Deutsche Forschungsgemeinschaft for financial support through SFB 491.

*christoph.hassel@uni-due.de

- ¹E. Abrahams, P. W. Anderson, D. C. Licciardello, and T. V. Ramakrishnan, *Phys. Rev. Lett.* **42**, 673 (1979).
- ²B. L. Altshuler, A. G. Aronov, and P. A. Lee, *Phys. Rev. Lett.* **44**, 1288 (1980).
- ³Y. Aharonov and D. Bohm, *Phys. Rev.* **115**, 485 (1959).
- ⁴D. Yu. Sharvin and Yu. V. Sharvin, *JETP Lett.* **34**, 272 (1981).
- ⁵G. Bergmann, *Phys. Rep.* **107**, 1 (1984).
- ⁶B. L. Altshuler and A. G. Aronov, in *Localization and Electron-Electron-Interactions in Disordered Systems*, edited by A. L. Efros and M. Pollak (North Holland, Amsterdam, 1985).
- ⁷H. Raffy, L. Dumoulin, and J. P. Burger, *Phys. Rev. B* **36**, 2158 (1987).
- ⁸M. Rubinstein, F. J. Rachford, W. W. Fuller, and G. A. Prinz, *Phys. Rev. B* **37**, 8689 (1988).
- ⁹M. Aprili, J. Lesueur, L. Dumoulin, and J. P. Nédellec, *Solid State Commun.* **102**, 41 (1997).
- ¹⁰F. G. Aliev, E. Kunnen, K. Temst, K. Mae, G. Verbanck, J. Barnas, V. V. Moshchalkov, and Y. Bruynseraede, *Phys. Rev. Lett.* **78**, 134 (1997).
- ¹¹T. Ono, Y. Ooka, S. Kasai, H. Mijayima, K. Mibu, and T. Shinjo, *J. Magn. Magn. Mater.* **226-230**, 1831 (2001).
- ¹²S. Kasai, T. Niiyama, E. Saitoh, and H. Miyayima, *Appl. Phys. Lett.* **81**, 316 (2002).
- ¹³K. Tsubaki, *Jpn. J. Appl. Phys., Part 2* **40**, 1902 (2001).
- ¹⁴G. Tatara, H. Kohno, E. Bonet, and B. Barbara, *Phys. Rev. B* **69**,

054420 (2004).

- ¹⁵G. Tatara and H. Fukuyama, *Phys. Rev. Lett.* **78**, 3773 (1997).
- ¹⁶V. K. Dugaev, P. Bruno, and J. Barnas, *Phys. Rev. B* **64**, 144423 (2001).
- ¹⁷F. G. Aliev, R. Schad, A. Volodin, K. Temst, C. van Haesendonck, Y. Bruynseraede, I. Vavra, V. K. Dugaev, and R. Villar, *Europhys. Lett.* **63**, 888 (2003).
- ¹⁸D. Neumaier, K. Wagner, S. Geiszler, U. Wurstbauer, J. Sadowski, W. Wegscheider, and D. Weiss, *Phys. Rev. Lett.* **99**, 116803 (2007).
- ¹⁹M. Brands, C. Hassel, A. Carl, and G. Dumpich, *Phys. Rev. B* **74**, 033406 (2006).
- ²⁰M. Brands, A. Carl, O. Posth, and G. Dumpich, *Phys. Rev. B* **72**, 085457 (2005).
- ²¹S. Sil, P. Entel, G. Dumpich, and M. Brands, *Phys. Rev. B* **72**, 174401 (2005).
- ²²C. Hassel, F. M. Römer, R. Meckenstock, G. Dumpich, and J. Lindner, *Phys. Rev. B* **77**, 224439 (2008).
- ²³M. Brands, R. Wieser, C. Hassel, D. Hinzke, and G. Dumpich, *Phys. Rev. B* **74**, 174411 (2006).
- ²⁴<http://math.nist.gov/oommf/>
- ²⁵R. McGuire and R. I. Potter, *IEEE Trans. Magn.* **11**, 1018 (1975).
- ²⁶G. Neuttiens, J. Eom, C. Strunk, V. Chandrasekhar, C. van Haesendonck, and Y. Bruynseraede, *Europhys. Lett.* **34**, 617 (1996).